

## Supporting Information

# Metal Ion Detection by Naphthylthiourea Derivatives through 'Turn-On' Excimer Emission

Chanchal Agarwal, Edamana Prasad\*

Department of Chemistry, Indian Institute of Technology Madras, Chennai 600 036, India

Fax: (+) 91-2257-4202, , Tel.: +91-44-2257-4232

E-mail: pre@iitm.ac.in

Contents	Page Number
1. UV-Visible absorption spectra of L1, L2 and L3 in presence of metal ions (Figure S1-S3) .....	03
2. UV-visible absorption spectra of L1 (75 $\mu\text{M}$ ) upon addition of $\text{Hg}^{2+}$ in DMSO (Figure S4).....	04
3. Excited state decay from L1 and L1 upon treating with $\text{Hg}^{2+}$ ion in DMSO (Figure S5 & S6).....	04
4. Job's plot between $\text{Hg}^{2+}$ and L1, L2 and L3 in DMSO (Figure S7-S9).....	04-05
5. Detection limit and EDAX spectrum of L1 upon treating with $\text{Hg}^{2+}$ (Figure S10-S11).....	05
6. UV-Visible absorption spectra of L2 and L3 in presence of $\text{Hg}^{2+}$ (Figure S12 & S13).....	06
7. Steady state fluorescence spectra of L2 and L3 in presence of $\text{Hg}^{2+}$ (Figure S14 & S15).....	06
8. Excited state decay from L2 and L3 upon treating with $\text{Hg}^{2+}$ ion in DMSO (Figure S16- S19).....	07
9. Detection limit of L2 and L3 upon treating with $\text{Hg}^{2+}$ (Figure S20-S21).....	08
10. Photophysical study of L1 in presence of $\text{Cu}^{2+}$ in DMSO (Figure S22-S24).....	09
11. UV-visible absorption spectra of L2 and L3 upon addition of $\text{Cu}^{2+}$ in DMSO (Figure S25 & S26).....	10
12. Steady state fluorescence spectra of L2 and L3 upon addition of $\text{Cu}^{2+}$ in DMSO (Figure S27 & S28).....	10
13. $^1\text{H}$ NMR experiment of L3 in $\text{DMSO-}d_6$ in the presence of $\text{Cu}^{2+}$ acetate (Figure S29).....	11
14. Job's plot between $\text{Cu}^{2+}$ and L2 and L3 in DMSO (Figure S30 and S31).....	11
15. Binding constant and detection limit of L2 and L3 in presence of $\text{Cu}^{2+}$ in DMSO (Figure S32-S35).....	12-13
16. Excited state decay from L2 in presence of $\text{Cu}^{2+}$ in DMSO (Figure S36).....	14
17. EDTA effect on L2- $\text{Cu}^{2+}$ and L3- $\text{Cu}^{2+}$ system in DMSO (Figure S37 & S38).....	14

18. UV-Visible of L2 and L3 in the presence of $\text{Co}^{2+}$ and $\text{Ag}^+$ respectively in DMSO (Figure S39-S40).....	14
19. Steady state fluorescence spectra and Job's plot in DMSO (Figure S41-S44).....	15
20. Excited state decay from L2 and L3 in presence of $\text{Co}^{2+}$ and $\text{Ag}^+$ , respectively in DMSO (Figure S45-S46).....	16
21. Binding constant of L2 in presence of $\text{Co}^{2+}$ in DMSO (Figure S47).....	16
22. Detection limit of L2 and L3 in presence of $\text{Co}^{2+}$ and $\text{Ag}^+$ ion (Figure S48-S49).....	16
23. $^1\text{H}$ NMR experiment of L2 and L3 in $\text{DMSO-}d_6$ in the presence of $\text{Ag}^+$ and $\text{Co}^{2+}$ , respectively (Figure S50 and S51).....	17
24. EDTA effect on L2- $\text{Co}^{2+}$ and L3- $\text{Ag}^+$ system in DMSO, respectively (Figure S52 & S53).....	18
25. Interference study (Figure S54-S59).....	18-19
26. UV-Visible absorption spectra of L1 in presence of metal ions in aqueous medium (Figure S60).....	20
27. Excited state decay from L1 and L1 in presence of $\text{Hg}^{2+}$ in aqueous medium (Figure S61 & S62).....	20
28. Steady state fluorescence spectra of L1 in presence of $\text{Hg}^{2+}$ in aqueous medium (Figure S63).....	21
29. Job's plot and detection limit study of L1 in presence of $\text{Hg}^{2+}$ in aqueous medium (Figure S64 & S65).....	21
30. Comparison experiment for the detection of $\text{Hg}^{2+}$ ion at room temperature and at low temperature (Figure S66).....	22

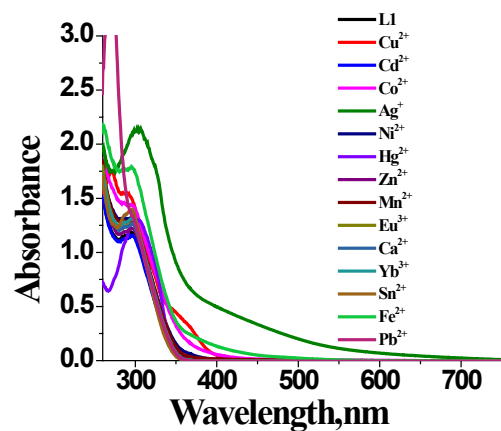


**Figure S1:** UV-visible absorption spectra of L1 (75 μM) upon addition of metal salts (3 equivalents) in DMSO.

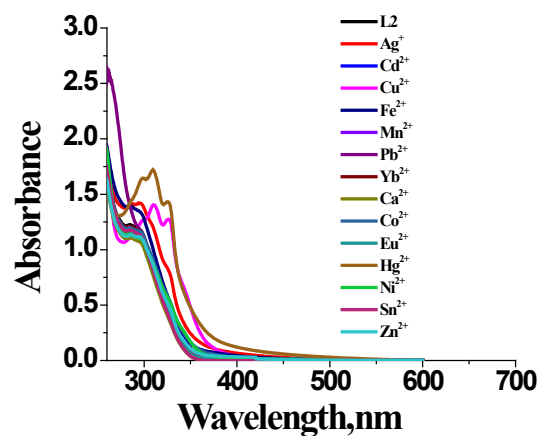


**Figure S2:** UV-visible absorption spectra of L2 (75 μM) upon addition of metal salts (1 equivalent) in DMSO.

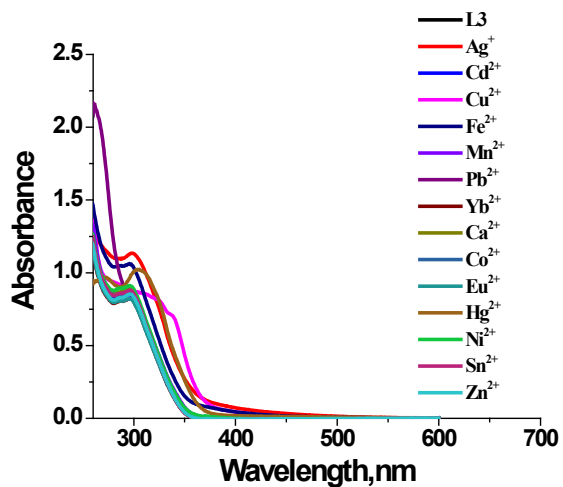


**Figure S3:** UV-visible absorption spectra of L3 (75 μM) upon addition of metal salts (1 equivalent) in DMSO.

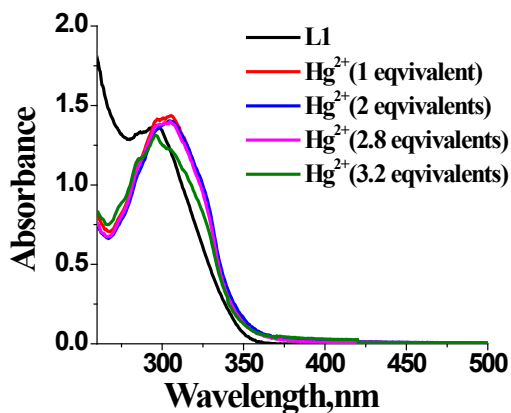


**Figure S4:** UV-visible absorption spectra of L1 (75 μM) upon addition of Hg<sup>2+</sup> (0-3 equivalents) in DMSO.

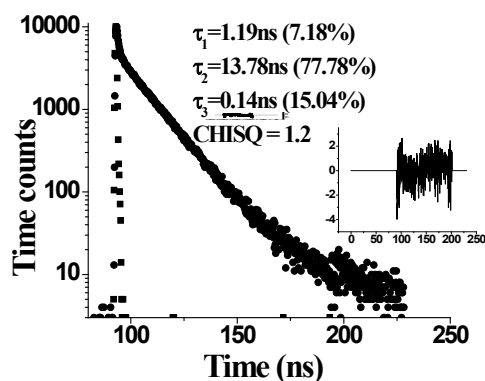


**Figure S5:** Excited state decay from L1 (75 μM) in DMSO. λ<sub>ex</sub> was 345 nm and emission was collected at 426 nm.

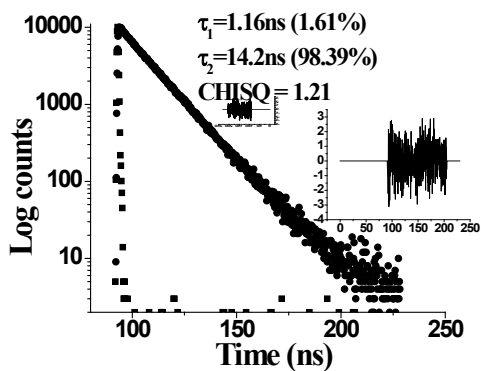


**Figure S6:** Excited state decay from L1 upon treating with Hg<sup>2+</sup> in DMSO. λ<sub>ex</sub> was 345 nm and emission was collected at 426 nm.

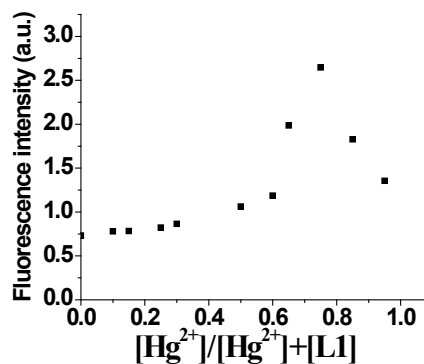


**Figure S7:** Fluorescence intensity has plotted with respect to mole fraction of [Hg<sup>2+</sup>]. Changes in fluorescence intensity band at 426 nm of L1 and Hg<sup>2+</sup> system with a total concentration of 75 μM in DMSO, indicating a 3:1 stoichiometric ratio of Hg<sup>2+</sup>:L1 (λ<sub>ex</sub> was 345 nm and λ<sub>em</sub> was 426 nm).

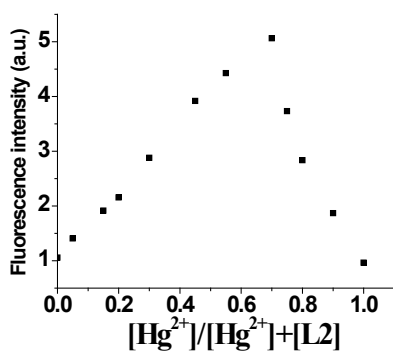


**Figure S8:** Fluorescence intensity has plotted with respect to mole fraction of  $[\text{Hg}^{2+}]$ . Changes in fluorescence intensity band at 426 nm of L2 and  $\text{Hg}^{2+}$  system with a total concentration of  $75\mu\text{M}$  in DMSO, indicating a 2:1 stoichiometric ratio of  $\text{Hg}^{2+}$ :L2 ( $\lambda_{\text{ex}}$  was 345 nm and  $\lambda_{\text{em}}$  was 426 nm).

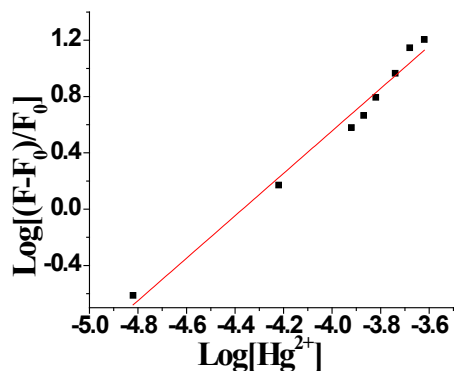


**Figure S10:** Plot of intensity of L1 ( $75\mu\text{M}$ ) with respect to  $[\text{Hg}^{2+}]$  ( $15\text{--}240\mu\text{M}$ ).  $\lambda_{\text{ex}}$  was 345 nm.

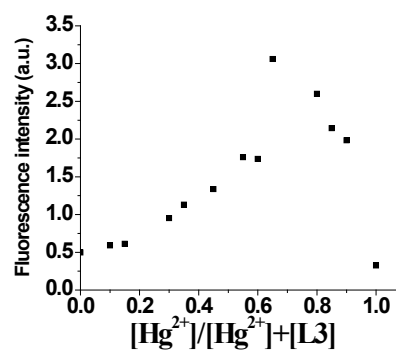


**Figure S9:** Fluorescence intensity has plotted with respect to mole fraction of  $[\text{Hg}^{2+}]$ . Changes in fluorescence intensity band at 426 nm of L3 and  $\text{Hg}^{2+}$  system with a total concentration of  $75\mu\text{M}$  in DMSO, indicating a 2:1 stoichiometric ratio of  $\text{Hg}^{2+}$ :L3 ( $\lambda_{\text{ex}}$  was 345 nm and  $\lambda_{\text{em}}$  was 426 nm).

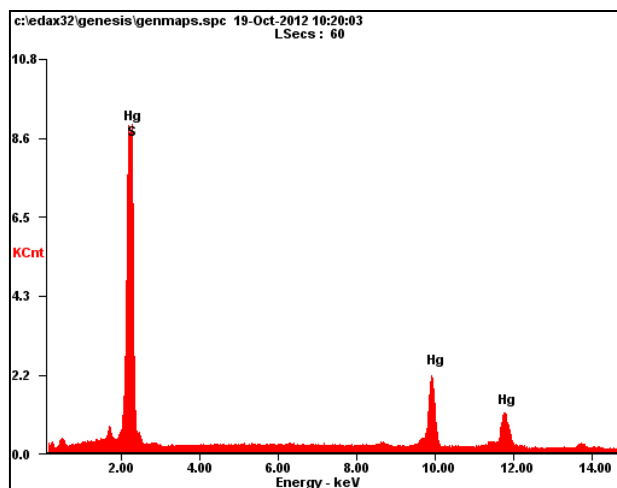


**Figure S11:** HgS formation upon addition of  $\text{Hg}^{2+}$  into L1 in DMSO was confirmed by EDAX

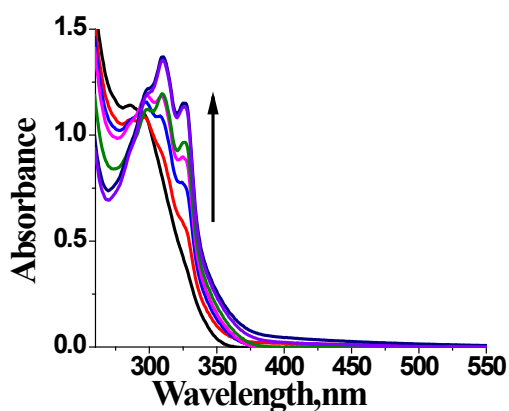


**Figure S12:** UV-visible absorption spectra of L2 (75 μM) upon addition of Hg<sup>2+</sup> (0-2 equivalents) in DMSO.

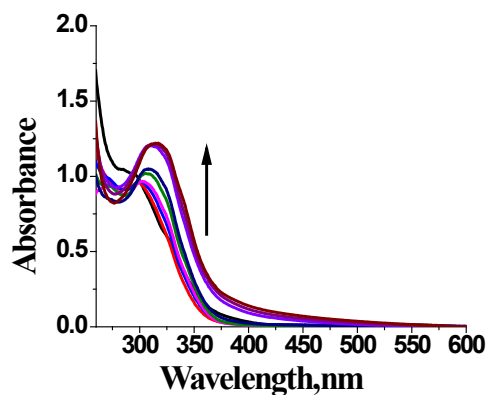


**Figure S13:** UV-visible absorption spectra of L3 (75 μM) upon addition of Hg<sup>2+</sup> (0-2 equivalents) in DMSO.

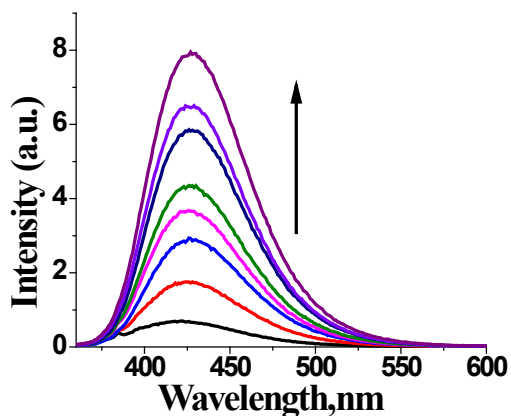


**Figure S14:** Steady state fluorescence spectra of L2 (75 μM) upon addition of Hg<sup>2+</sup> (2 equivalents) in DMSO.  $\lambda_{\text{ex}}$  was 345 nm.

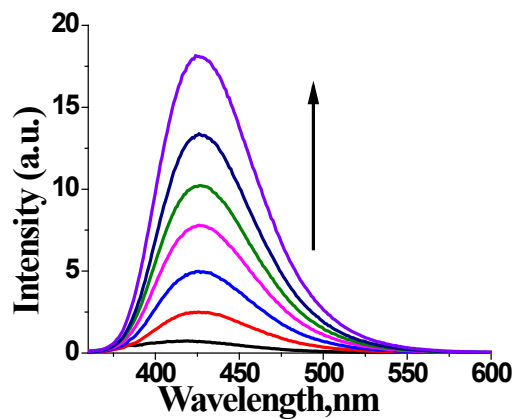


**Figure S15:** Steady state fluorescence spectra of L3 (75 μM) upon addition of Hg<sup>2+</sup> (3 equivalents) in DMSO.  $\lambda_{\text{ex}}$  was 345 nm.

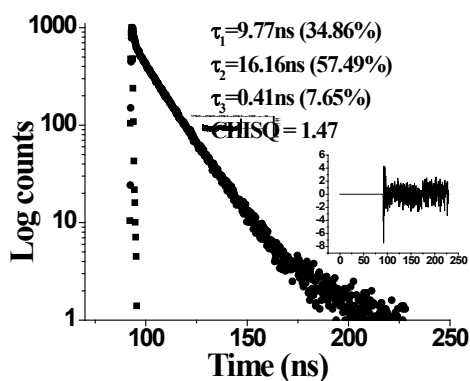


**Figure S16:** Excited state decay from L2 (75  $\mu\text{M}$ ) in DMSO.  $\lambda_{\text{ex}}$  was 345 nm and emission was collected at 426 nm.

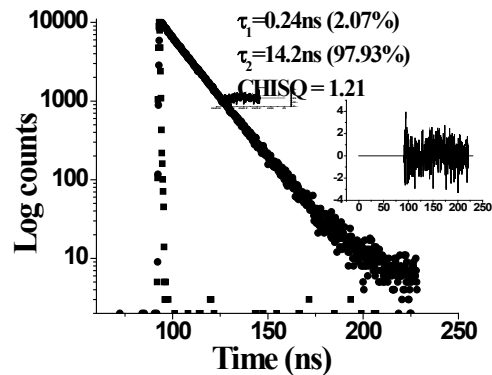


**Figure S17:** Excited state decay from L2 upon treating with  $\text{Hg}^{2+}$  in DMSO.  $\lambda_{\text{ex}}$  was 345 nm and emission was collected at 426 nm.

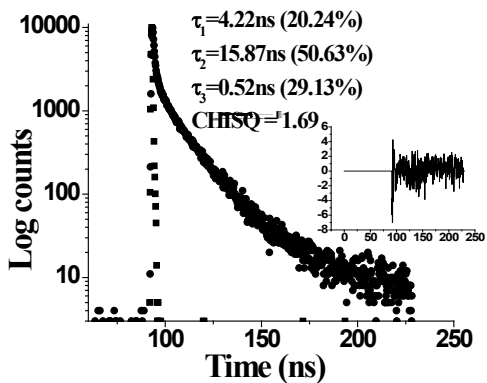


**Figure S18:** Excited state decay from L3 (75  $\mu\text{M}$ ) in DMSO.  $\lambda_{\text{ex}}$  was 345 nm and emission was collected at 426 nm.

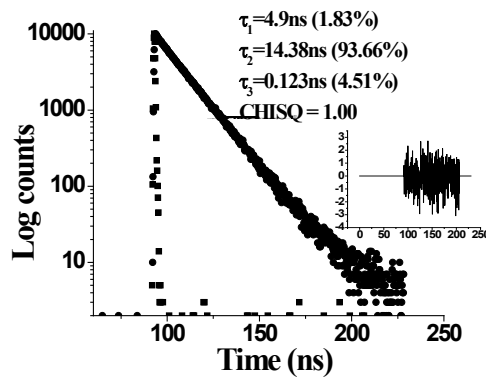


**Figure S19:** Excited state decay from L3 upon treating with  $\text{Hg}^{2+}$  in DMSO.  $\lambda_{\text{ex}}$  was 345 nm and emission was collected at 426 nm.

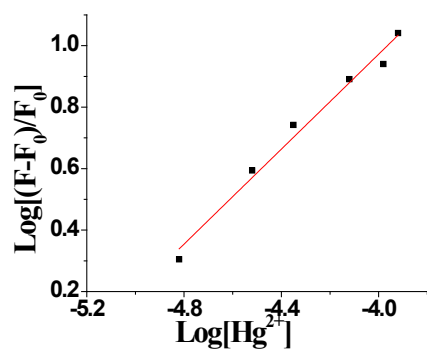


**Figure S20:** Plot of intensity of L2 (75  $\mu\text{M}$ ) with respect to  $[\text{Hg}^{2+}]$  (15-120  $\mu\text{M}$ ).  $\lambda_{\text{ex}}$  was 345 nm.

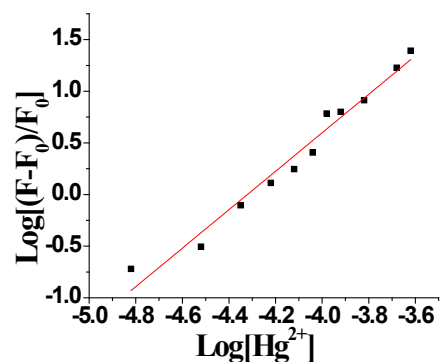


**Figure S21:** Plot of intensity of L3 (75  $\mu\text{M}$ ) with respect to  $[\text{Hg}^{2+}]$  (15-240  $\mu\text{M}$ ) in DMSO.  $\lambda_{\text{ex}}$  was 345 nm.



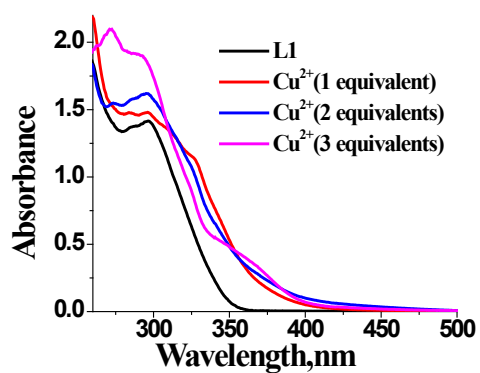


**Figure S22:** UV-visible absorption spectra of L1 (75 μM) upon addition of Cu<sup>2+</sup> (0-3 equivalents) in DMSO.

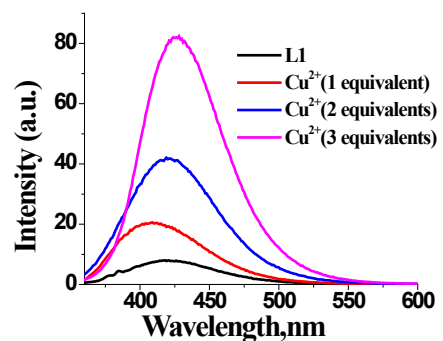


**Figure S23:** Steady state fluorescence spectra of L1 (75 μM) upon addition of Cu<sup>2+</sup> (0-3 equivalents) in DMSO.  $\lambda_{\text{exc}}$  was 345 nm.

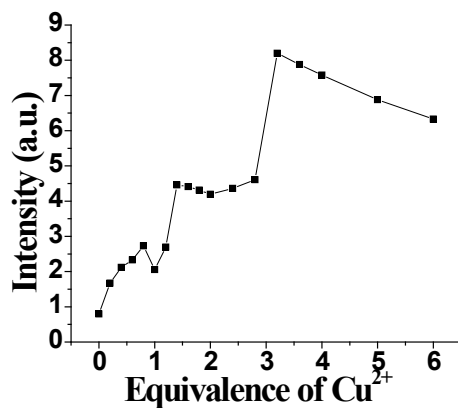


**Figure S24:** Plot of emission titration profile of L1 (75 μM) as a function of gradual addition of 0-6 equivalents (0-450 μM) of Cu<sup>2+</sup> in DMSO showing the non linear increment in the fluorescence intensity.  $\lambda_{\text{exc}}$ =345nm.

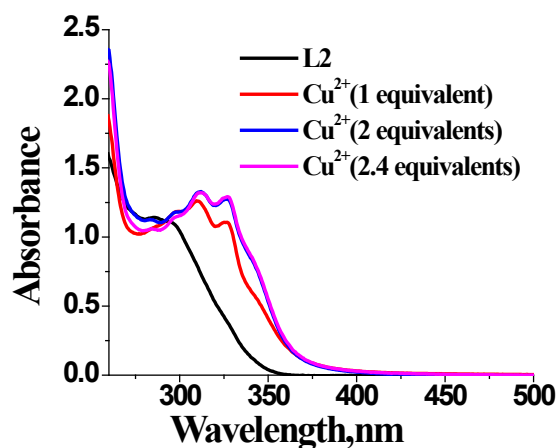


**Figure S25:** UV-visible absorption spectra of L2 (75 μM) upon addition of Cu<sup>2+</sup> (0- 2.4 equivalents) in DMSO.

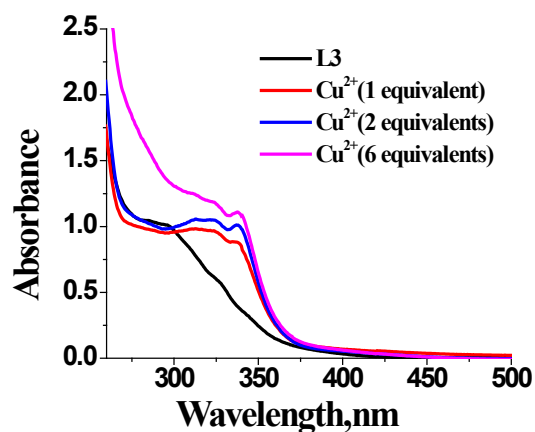


**Figure S26:** UV-visible absorption spectra of L3 (75 μM) upon addition of Cu<sup>2+</sup> (0-6 equivalents) in DMSO.

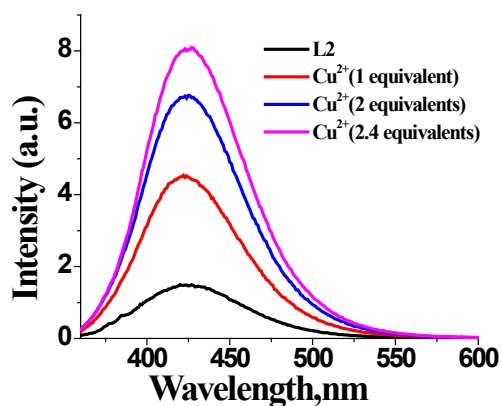


**Figure S27:** Steady state fluorescence spectra of L2 (75 μM) upon addition of Cu<sup>2+</sup> (0- 2.4 equivalents) in DMSO.  $\lambda_{\text{ex}}$  was 345 nm.

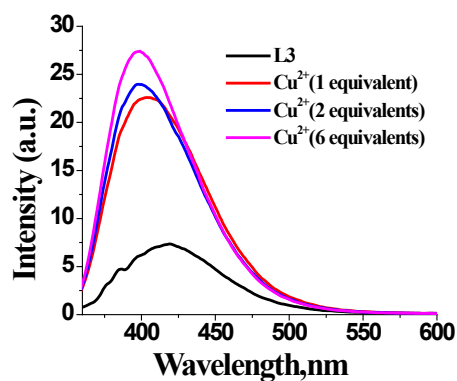


**Figure S28:** Steady state fluorescence spectra of L3 (75 μM) upon addition of Cu<sup>2+</sup> (0- 6 equivalents) in DMSO.  $\lambda_{\text{ex}}$  was 345 nm.

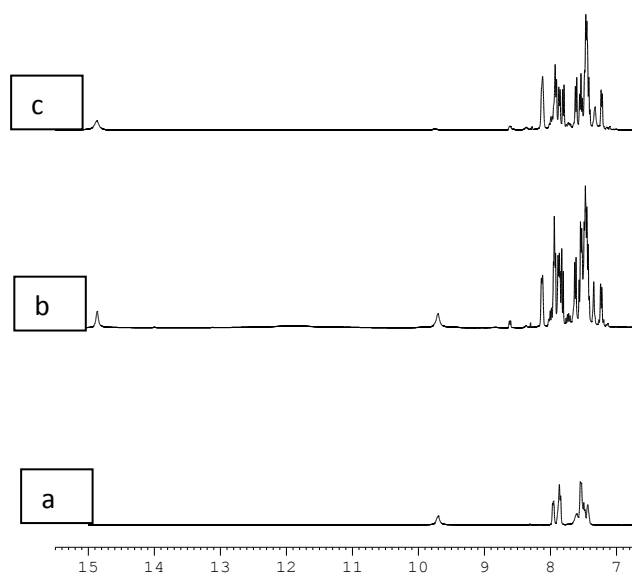


**Figure S29:**  $^1\text{H}$  NMR experiment of L3 in  $\text{DMSO-}d_6$  in the absence of  $\text{Cu}^{2+}$  acetate (spectrum a) and after the addition of 1 equivalents (spectrum b), 2.0 equivalents (spectrum c).

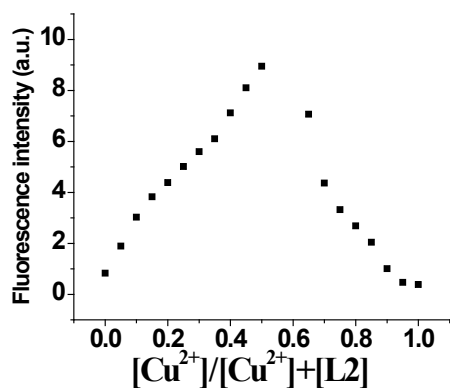


**Figure S30:** Job's plot between  $\text{Cu}^{2+}$  and L2 in DMSO. It confirms 1:1 binding mode.

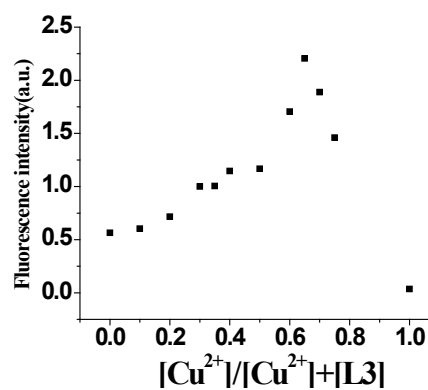


**Figure S31:** Job's plot between  $\text{Cu}^{2+}$  and L3 in DMSO. It confirms 2:1 binding mode.

### Binding constant determination by Modified Tsien equation:

The stoichiometry between  $\text{Cu}^{2+}$  ions and L3 is 2:1 which has been calculated by using Job's method. Equation 1 shows complex formation between  $\text{Cu}^{2+}$  ions (B) and L1 (A). The ratio between  $\text{Cu}^{2+}$  ions and L1 is m:n.



where  $K$  is the equilibrium constant of the reaction. According to the modified Stern-Volmer equation, the relationship between the change in the fluorescence intensities, the concentration of  $\text{Cu}^{2+}$  [B] and the total concentration of L1 [A] can be expressed as follows:

$$\frac{F_0 - F}{F} = K[A]^{n-1}B^m \quad (2)$$

suppose the change in the fluorescence intensities ( $\Delta F$ ) =  $F_0 - F$ , the equation 2 will be

$$\log(\Delta F/F) = \log k + (n - 1)\log[A] + m\log[B], \quad (3)$$

Where  $F_0$  and  $F$  represent the fluorescence intensities of L1 in the absence and in the presence of  $\text{Cu}^{2+}$ , respectively. The relative fluorescence intensity,  $\alpha$ , can be experimentally determined by measuring the fluorescence intensity,

$$\alpha = \frac{F - F_1}{F_0 - F_1} \quad (4)$$

Here,  $F$  is the fluorescence intensity of L1 in presence of different equivalent of  $\text{Cu}^{2+}$ .  $F_1$  is the maximum fluorescence intensity of L1- $\text{Cu}^{2+}$  system.  $F_0$  is the fluorescence intensity of L1 and the relationship between  $\alpha$  and  $\text{Cu}^{2+}$  concentrations can be shown by modified Tsien equation

$$[M^{n+}]^m = \frac{1}{n \cdot K} \cdot \frac{1}{[L]_T^{n-1}} \cdot \frac{1 - \alpha}{\alpha^n} \quad (5)$$

$n$  is the charge on the metal ion.  $m$  is the number of metal ion bound to the ligand. [L] is the concentration of the ligand. The response of L1 with different concentrations of  $\text{Cu}^{2+}$  has been fitted by using equation 5.

### The binding constant $K$ determination by the Benesi-Hildebrand equation

The binding constant  $K$  for L2-  $\text{Cu}^{2+}$  system was determined by the Benesi-Hildebrand equation. Based on the assumption that the fluorescence change is only induced by the formation of a 1:1 complex between L2 and metal ion (M), the equilibrium can be expressed by the following equations:

$$1/(F - F_0) = 1/\{K(F_{max} - F_0)[\text{Cu}^{2+}]\} + 1/(F_{max} - F_0) \quad (6)$$

where  $F_0$  is the fluorescence intensity of L2 in absence of  $\text{Cu}^{2+}$ ,  $F$  is the fluorescence intensity of L2 at any given  $\text{Cu}^{2+}$  concentration and  $F_{\text{max}}$  is the maximum fluorescence intensity of L2 in presence of  $\text{Cu}^{2+}$  in solution. The association constant  $K$  was evaluated graphically by plotting  $1/(F - F_0)$  against  $1/[\text{Cu}^{2+}]$ . Binding constant was obtained from the slope and intercept.

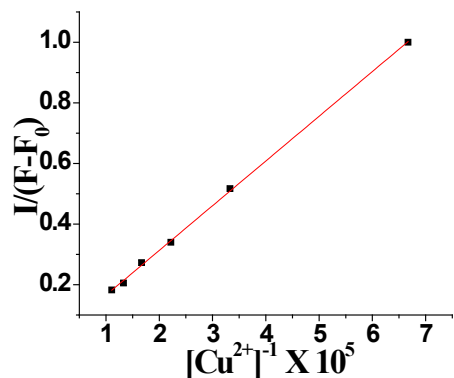


**Figure S32:** Benesi-Hildebrand plot of L2 with  $\text{Cu}^{2+}$  ions assuming 1:1 binding stoichiometry in DMSO.

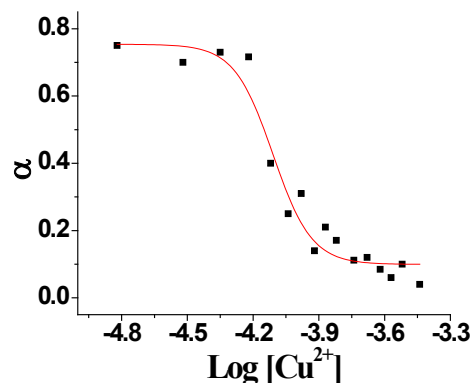


**Figure S33:** Response parameter values ( $\alpha$ ) vs  $\log [\text{Cu}^{2+}]$  for L3 in DMSO.

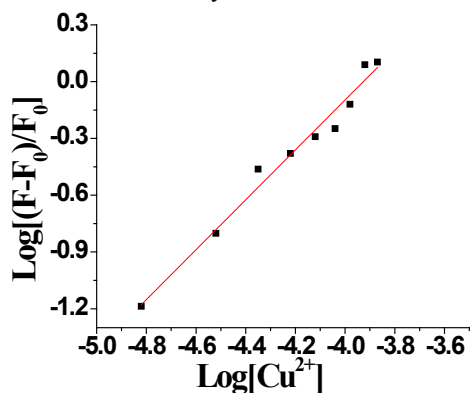


**Figure S34:** Plot of intensity of L2 ( $75\mu\text{M}$ ) with respect to  $[\text{Cu}^{2+}]$  ( $15\text{-}135\mu\text{M}$ ).  $\lambda_{\text{ex}}$  was  $345\text{ nm}$ .

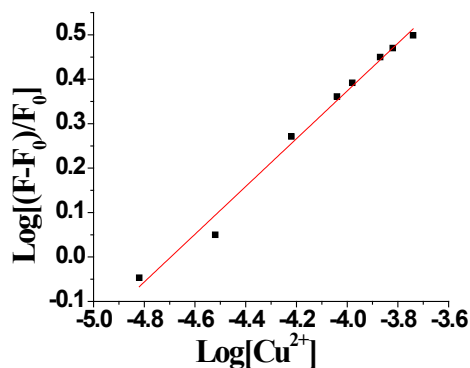


**Figure S35:** Plot of intensity of L3 ( $75\mu\text{M}$ ) with respect to  $[\text{Cu}^{2+}]$  ( $15\text{-}180\mu\text{M}$ ) in DMSO.  $\lambda_{\text{ex}}$  was  $345\text{ nm}$ .

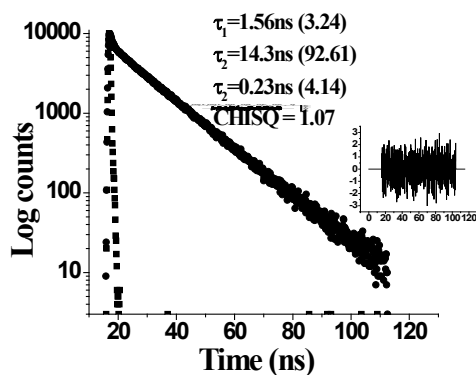


**Figure S36:** Excited state decay from L2 (75 μM) in presence of Cu<sup>2+</sup> in DMSO.  $\lambda_{\text{ex}}$  was 345 nm and emission was collected at 426 nm.

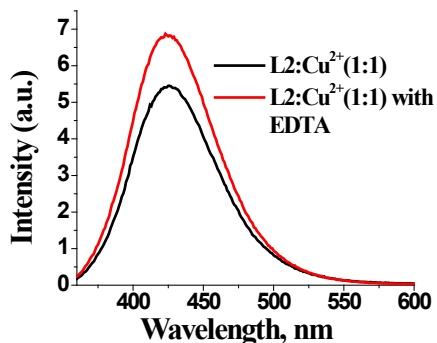


**Figure S37:** EDTA (5 equivalents) effect on L2-Cu<sup>2+</sup> system in DMSO.

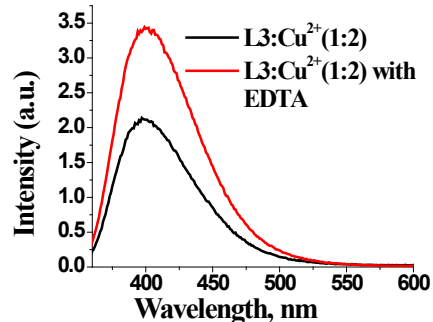


**Figure S38:** EDTA (5 equivalents) effect on L3-Cu<sup>2+</sup> system in DMSO.

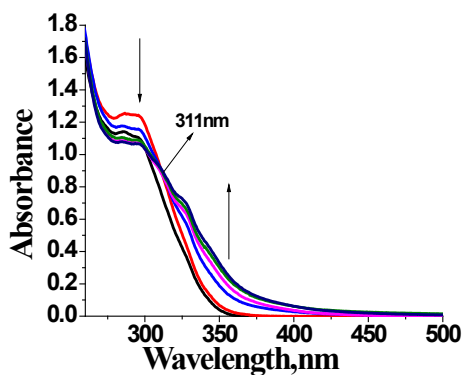


**Figure S39:** UV-visible absorption spectra of L2 (75 μM) upon addition of Co<sup>2+</sup> (1 equivalent) in DMSO.

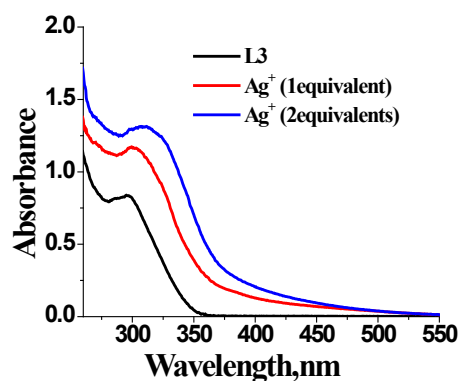


**Figure S40:** UV-visible absorption spectra of L3 (75 μM) upon addition of Ag<sup>+</sup> (2 equivalents) in DMSO.

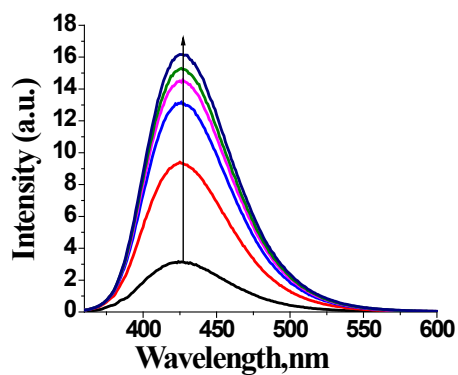


**Figure S41:** Steady state fluorescence spectra of L2 (75 μM) upon addition of Co<sup>2+</sup> (1 equivalent) in DMSO.  $\lambda_{\text{ex}}$  was 345 nm.  $\lambda_{\text{em}}$  was 429 nm.

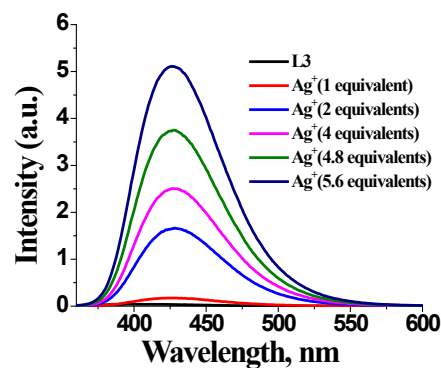


**Figure S42:** Steady state fluorescence spectra of L3 (75 μM) upon addition of Ag<sup>+</sup> (0-5.6 equivalents) in DMSO.  $\lambda_{\text{ex}}$  was 345 nm.

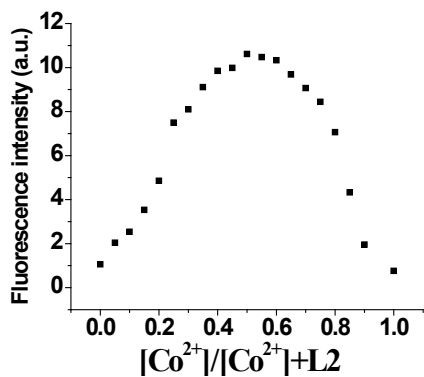


**Figure S43:** Job's plot between Co<sup>2+</sup> and L2 in DMSO. It confirms 1:1 binding mode.

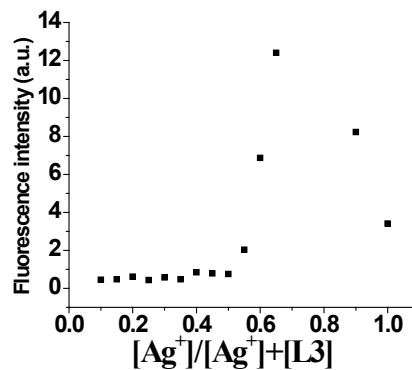


**Figure S44:** Job's plot between Ag<sup>+</sup> and L3 in DMSO. It confirms 2:1 binding mode.

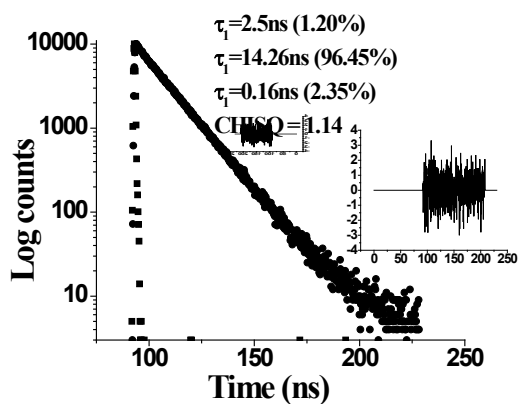


**Figure S45:** Excited state decay from L2 (75 μM) in presence of Co<sup>2+</sup> in DMSO.  $\lambda_{\text{ex}}$  was 345 nm and emission was collected at 426 nm.

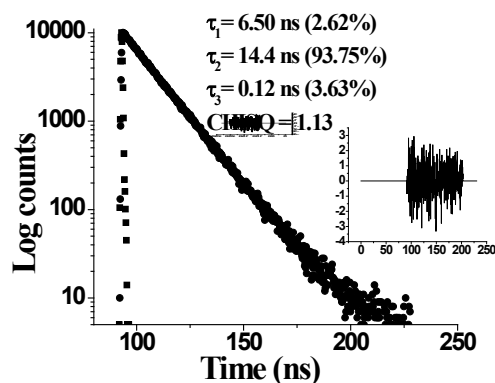


**Figure S46:** Excited state decay from L3 (75 μM) in presence of Ag<sup>+</sup> in DMSO.  $\lambda_{\text{ex}}$  was 345 nm and emission was collected at 426 nm.

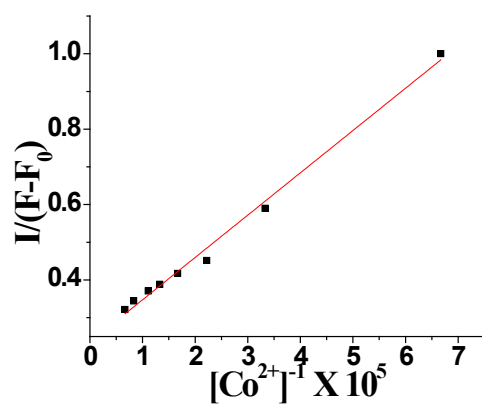


**Figure S47:** Benesi-Hildebrand plot of L2 with Co<sup>2+</sup> assuming 1:1 binding stoichiometry in DMSO.

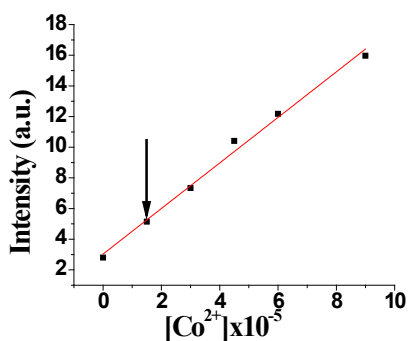


**Figure S48:** Plot of intensity of L2 (75 μM) with respect to [Co<sup>2+</sup>] (30-180 μM).  $\lambda_{\text{ex}}$  was 345 nm.

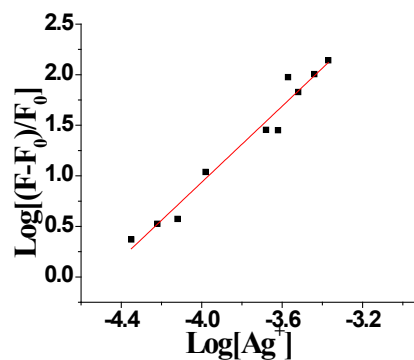


**Figure S49:** Plot of intensity of L3 (75 μM) with respect to [Ag<sup>+</sup>] (45-420 μM) in DMSO.  $\lambda_{\text{ex}}$  was 345 nm.



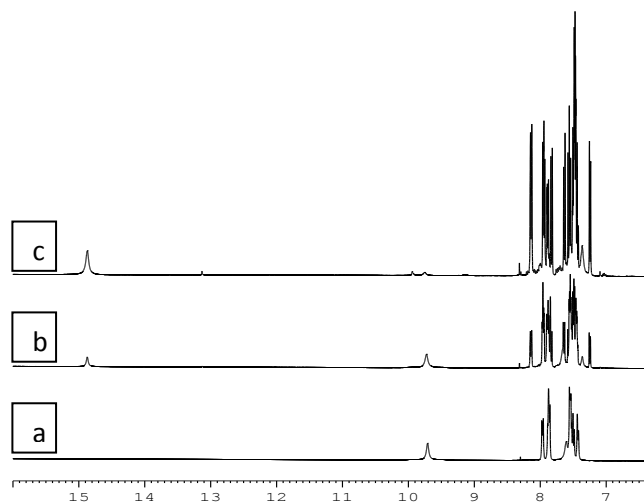


**Figure S50:**  $^1\text{H}$  NMR experiment of L3 in  $\text{DMSO-}d_6$  in the absence of  $\text{Ag}^+$  acetate (spectrum a) and after the addition of 1.0 equivalent (spectrum b) and 2.0 equivalents of silver (spectrum c).

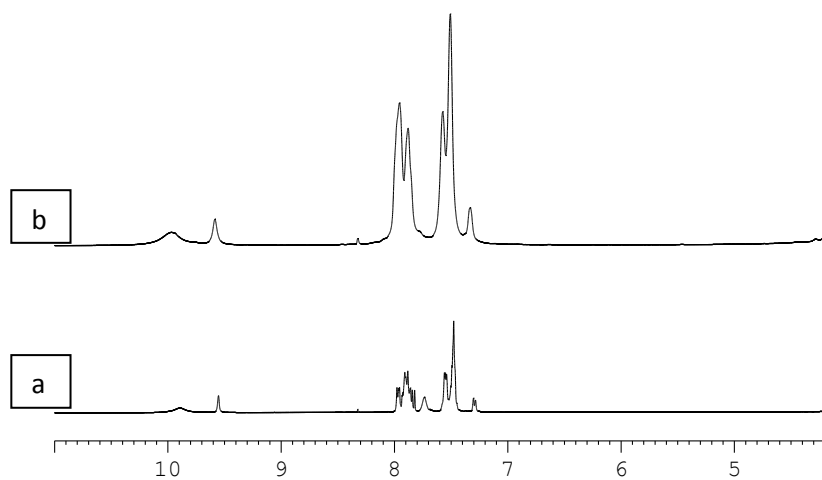


**Figure S51:**  $^1\text{H}$  NMR experiment of L2 in  $\text{DMSO-}d_6$  in the absence of  $\text{Co}^{2+}$  acetate (spectrum a) and after the addition of 1.0 equivalent (spectrum b).

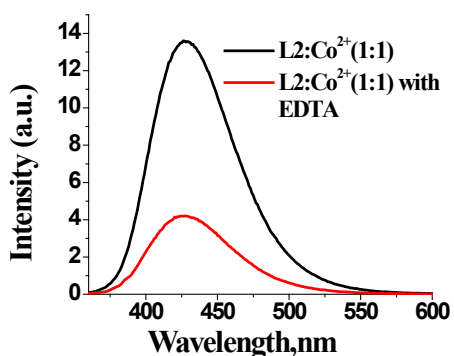


**Figure S52:** EDTA (5 equivalents) effect on metal ligand complex in DMSO.

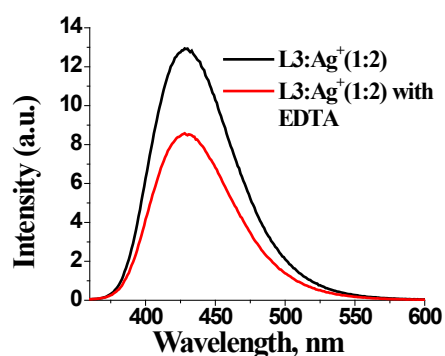


**Figure S53:** EDTA (5 equivalents) effect on metal ligand complex in DMSO.

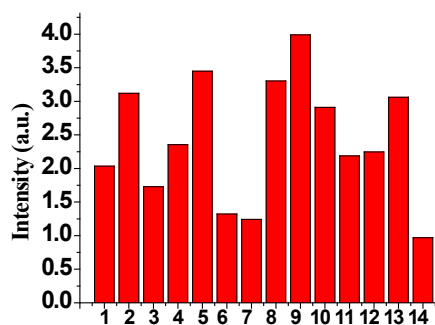


**Figure S54:** The fluorescence response from L1- $\text{Hg}^{2+}$  ( $75\mu\text{M}$ ) upon addition of 3 equiv. cation of interest: 1, L1- $\text{Hg}^{2+}$ ; 2,  $\text{Hg}^{2+}$ - $\text{Yb}^{3+}$ ; 3,  $\text{Hg}^{2+}$ - $\text{Cu}^{2+}$ ; 4,  $\text{Hg}^{2+}$ - $\text{Sn}^{2+}$ ; 5,  $\text{Hg}^{2+}$ - $\text{Mn}^{2+}$ ; 6,  $\text{Hg}^{2+}$ - $\text{Cd}^{2+}$ ; 7,  $\text{Hg}^{2+}$ - $\text{Ag}^{+}$ ; 8,  $\text{Hg}^{2+}$ - $\text{Eu}^{3+}$ ; 9,  $\text{Hg}^{2+}$ - $\text{Co}^{2+}$ ; 10,  $\text{Hg}^{2+}$ - $\text{Ni}^{2+}$ ; 11,  $\text{Hg}^{2+}$ - $\text{Ca}^{2+}$ ; 12,  $\text{Hg}^{2+}$ - $\text{Fe}^{2+}$ ; 13,  $\text{Hg}^{2+}$ - $\text{Zn}^{2+}$ ; 14,  $\text{Hg}^{2+}$ - $\text{Pb}^{2+}$  in DMSO.  $\lambda_{\text{ex}}$  was 345 nm.

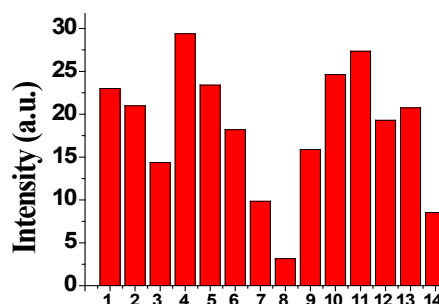


**Figure S55:** The fluorescence response from L2- $\text{Hg}^{2+}$  ( $75\mu\text{M}$ ) upon addition of 8 equiv. cation of interest: 1, L2- $\text{Hg}^{2+}$ ; 2,  $\text{Hg}^{2+}$ - $\text{Ni}^{2+}$ ; 3,  $\text{Hg}^{2+}$ - $\text{Ag}^{+}$ ; 4,  $\text{Hg}^{2+}$ - $\text{Co}^{2+}$ ; 5,  $\text{Hg}^{2+}$ - $\text{Yb}^{2+}$ ; 6,  $\text{Hg}^{2+}$ - $\text{Ca}^{2+}$ ; 7,  $\text{Hg}^{2+}$ - $\text{Cu}^{2+}$ ; 8,  $\text{Hg}^{2+}$ - $\text{Pb}^{2+}$ ; 9,  $\text{Cu}^{2+}$ - $\text{Sn}^{2+}$ ; 10,  $\text{Cu}^{2+}$ - $\text{Cd}^{2+}$ ; 11,  $\text{Cu}^{2+}$ - $\text{Mn}^{2+}$ ; 12,  $\text{Cu}^{2+}$ - $\text{Zn}^{2+}$ ; 13,  $\text{Cu}^{2+}$ - $\text{Eu}^{3+}$ ; 14,  $\text{Cu}^{2+}$ - $\text{Fe}^{2+}$  in DMSO.  $\lambda_{\text{ex}}$  was 345 nm.

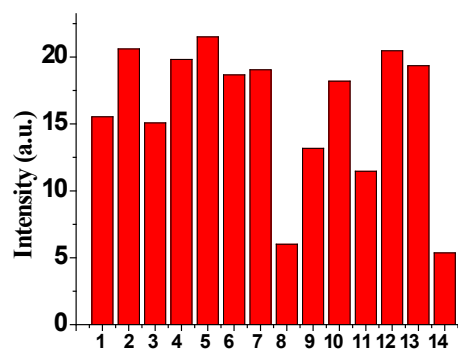


**Figure S56:** The fluorescence response from L2-Cu<sup>2+</sup> (75μM) upon addition of 8 equiv. cation of interest: 1, L2-Cu<sup>2+</sup>; 2, Cu<sup>2+</sup>-Ni<sup>2+</sup>; 3, Cu<sup>2+</sup>-Ag<sup>+</sup>; 4, Cu<sup>2+</sup>-Co<sup>2+</sup>; 5, Cu<sup>2+</sup>-Yb<sup>2+</sup>; 6, Cu<sup>2+</sup>-Ca<sup>2+</sup>; 7, Cu<sup>2+</sup>-Hg<sup>2+</sup>; 8, Cu<sup>2+</sup>-Pb<sup>2+</sup>; 9, Hg<sup>2+</sup>-Sn<sup>2+</sup>; 10, Hg<sup>2+</sup>-Cd<sup>2+</sup>; 11, Hg<sup>2+</sup>-Mn<sup>2+</sup>; 12, Hg<sup>2+</sup>-Zn<sup>2+</sup>; 13, Hg<sup>2+</sup>-Eu<sup>3+</sup>; 14, Hg<sup>2+</sup>-Fe<sup>2+</sup> in DMSO. λ<sub>ex</sub> was 345 nm.

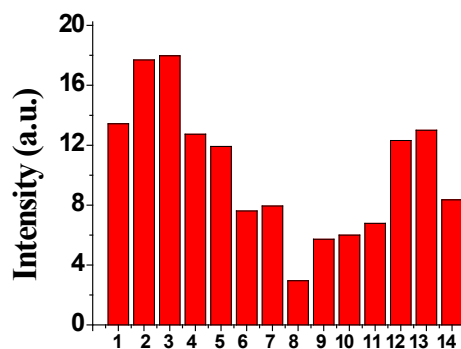


**Figure S57:** The fluorescence response from L3-Cu<sup>2+</sup> (75μM) upon addition of 2 equiv. cation of interest: 1, L1-Cu<sup>2+</sup>; 2, Cu<sup>2+</sup>-Ni<sup>2+</sup>; 3, Cu<sup>2+</sup>-Ag<sup>+</sup>; 4, Cu<sup>2+</sup>-Co<sup>2+</sup>; 5, Cu<sup>2+</sup>-Yb<sup>2+</sup>; 6, Cu<sup>2+</sup>-Ca<sup>2+</sup>; 7, Cu<sup>2+</sup>-Hg<sup>2+</sup>; 8, Cu<sup>2+</sup>-Pb<sup>2+</sup>; 9, Cu<sup>2+</sup>-Sn<sup>2+</sup>; 10, Cu<sup>2+</sup>-Cd<sup>2+</sup>; 11, Cu<sup>2+</sup>-Mn<sup>2+</sup>; 12, Cu<sup>2+</sup>-Zn<sup>2+</sup>; 13, Cu<sup>2+</sup>-Eu<sup>3+</sup>; 14, Cu<sup>2+</sup>-Fe<sup>2+</sup> in DMSO. λ<sub>ex</sub> was 345 nm.

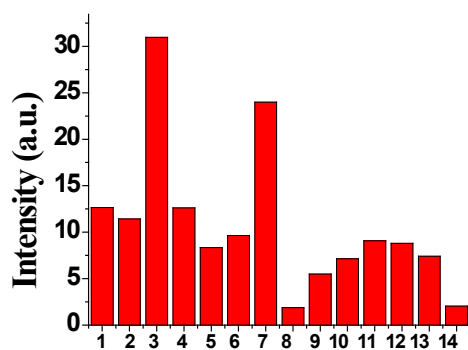


**Figure S59:** The fluorescence response from L2-Co<sup>2+</sup> (75μM) upon addition of 8 equiv. cation of interest: 1, L2-Co<sup>2+</sup>; 2, Co<sup>2+</sup>-Ni<sup>2+</sup>; 3, Co<sup>2+</sup>-Ag<sup>+</sup>; 4, Co<sup>2+</sup>-Cu<sup>2+</sup>; 5, Co<sup>2+</sup>-Yb<sup>2+</sup>; 6, Co<sup>2+</sup>-Ca<sup>2+</sup>; 7, Co<sup>2+</sup>-Hg<sup>2+</sup>; 8, Co<sup>2+</sup>-Pb<sup>3+</sup>; 9, Co<sup>2+</sup>-Sn<sup>2+</sup>; 10, Co<sup>2+</sup>-Cd<sup>2+</sup>; 11, Co<sup>2+</sup>-Mn<sup>2+</sup>; 12, Co<sup>2+</sup>-Zn<sup>2+</sup>; 13, Co<sup>2+</sup>-Eu<sup>3+</sup>; 14, Co<sup>2+</sup>-Fe<sup>2+</sup> in DMSO. λ<sub>ex</sub> was 345 nm.

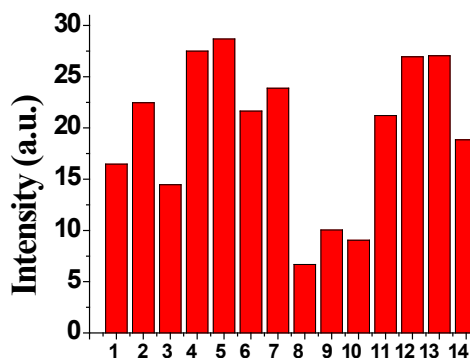


**Figure S58:** The fluorescence response from L3-Ag<sup>+</sup> (75μM) upon addition of 2 equiv. cation of interest: 1, L1-Ag<sup>+</sup>; 2, Ag<sup>+</sup>-Ni<sup>2+</sup>; 3, Ag<sup>+</sup>-Cu<sup>2+</sup>; 4, Ag<sup>+</sup>-Co<sup>2+</sup>; 5, Ag<sup>+</sup>-Yb<sup>2+</sup>; 6, Ag<sup>+</sup>-Ca<sup>2+</sup>; 7, Ag<sup>+</sup>-Hg<sup>2+</sup>; 8, Ag<sup>+</sup>-Pb<sup>2+</sup>; 9, Ag<sup>+</sup>-Sn<sup>2+</sup>; 10, Ag<sup>+</sup>-Cd<sup>2+</sup>; 11, Ag<sup>+</sup>-Mn<sup>2+</sup>; 12, Ag<sup>+</sup>-Zn<sup>2+</sup>; 13, Ag<sup>+</sup>-Eu<sup>3+</sup>; 14, Ag<sup>+</sup>-Fe<sup>2+</sup> in DMSO. λ<sub>ex</sub> was 345 nm.

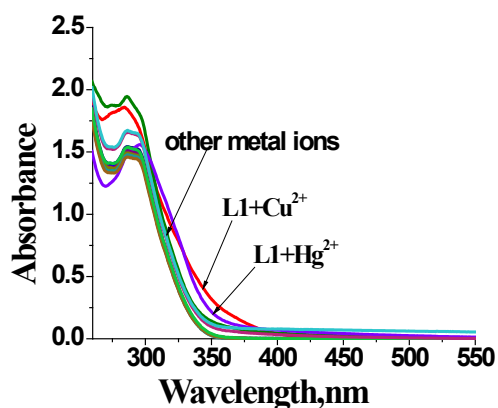


**Figure S60:** UV-visible absorption spectra of L1 (75  $\mu\text{M}$ ) upon addition of  $\text{Ag}^+$ ,  $\text{Ca}^{2+}$ ,  $\text{Cd}^{2+}$ ,  $\text{Co}^{2+}$ ,  $\text{Fe}^{2+}$ ,  $\text{Hg}^{2+}$ ,  $\text{Mn}^{2+}$ ,  $\text{Ni}^{2+}$ ,  $\text{Pb}^{2+}$ ,  $\text{Cu}^{2+}$ ,  $\text{Sn}^{2+}$ ,  $\text{Zn}^{2+}$ ,  $\text{Yb}^{3+}$  and  $\text{Eu}^{3+}$  (1 equivalent) in aqueous medium (10mM HEPES, 60% DMSO, pH=7.2).

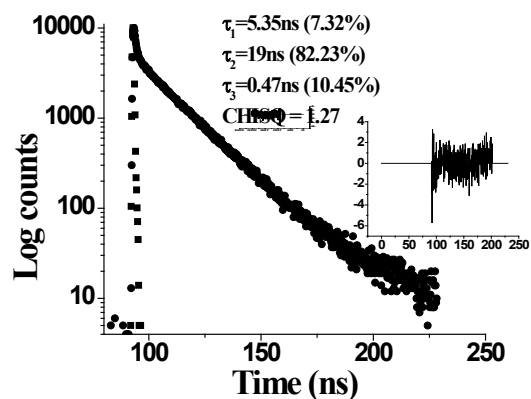


**Figure S61:** Excited state decay from L1 (75  $\mu\text{M}$ ) in aqueous medium (10mM HEPES, 60% DMSO, pH=7.2).  $\lambda_{\text{ex}}$  was 345 nm and emission was collected at 426 nm.

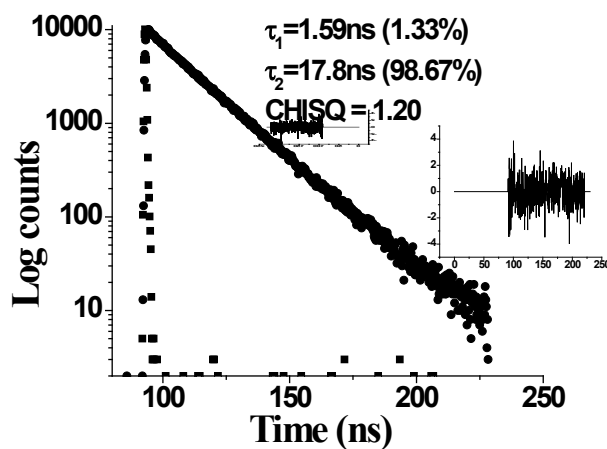


**Figure S62:** Excited state decay from L1 upon treating with  $\text{Hg}^{2+}$  in aqueous medium (10mM HEPES, 60% DMSO, pH=7.2).  $\lambda_{\text{ex}}$  was 345 nm and emission was collected at 426 nm.

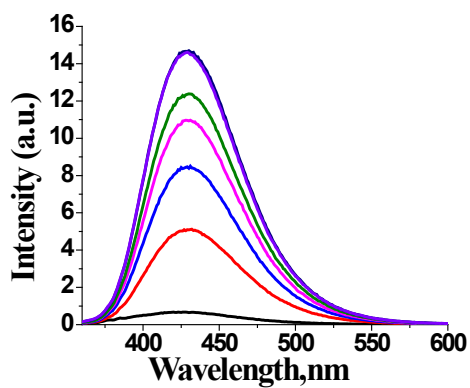


**Figure S63:** Steady state fluorescence spectra of L1 (75 $\mu$ M) upon addition of Hg<sup>2+</sup> (0-8 equivalents) in aqueous medium (10mM HEPES, 60% DMSO, pH=7.2).  $\lambda_{\text{ex}}$  was 345 nm.

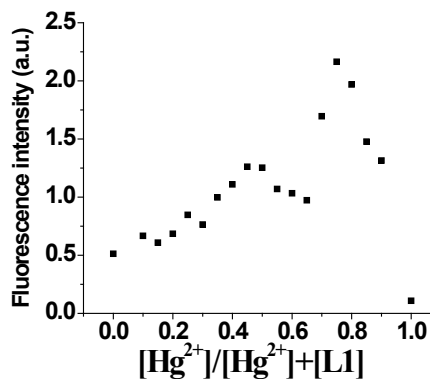


**Figure S64:** Job's plot between Hg<sup>2+</sup> and L1 in aqueous medium (10mM HEPES, 60% DMSO, pH=7.2). It confirms 3:1 binding mode.

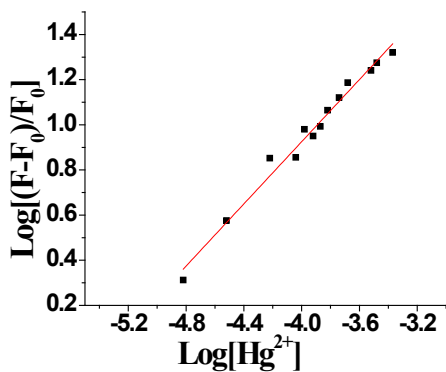


**Figure S65:** Plot of intensity of L1 (75 $\mu$ M) with respect to [Hg<sup>2+</sup>] (15-420  $\mu$ M) in aqueous medium (10mM HEPES, 60% DMSO, pH=7.2).  $\lambda_{\text{ex}}$  was 345 nm.

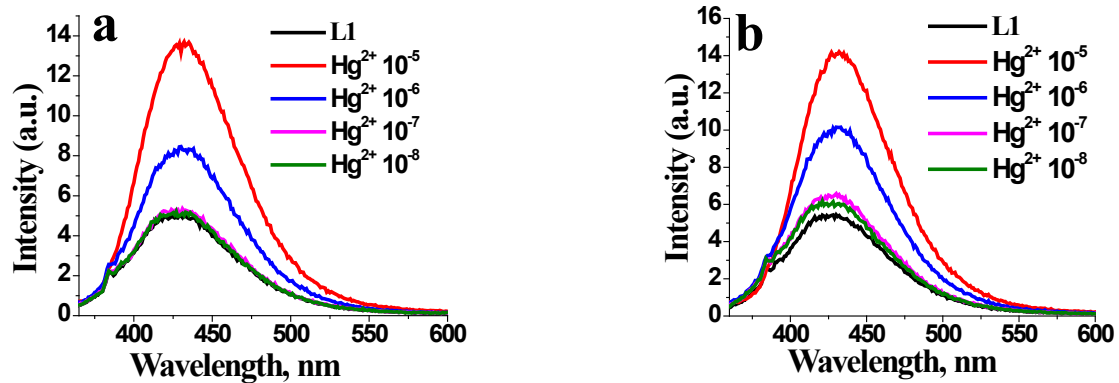


**Figure S66:** Steady state fluorescence spectra of L1 (75 μM) upon addition of Hg<sup>2+</sup> ( $7.5 \times 10^{-5}$ - $7.5 \times 10^{-8}$  M) (a) at room temperature and (b) at 5 °C in aqueous medium (10 mM HEPES, 60% DMSO, pH=7.2).  $\lambda_{\text{ex}}$  was 345 nm.